

1  
2  
3  
4  
5  
6  
7  
8  
9  
10  
11  
12  
13  
14  
15  
16  
17  
18  
19  
20  
21  
22  
23

*Geophysical Research Letters*

Supporting Information for

**A more general paradigm for understanding the decoupling of stratocumulus-topped boundary layers: the importance of horizontal temperature advection**

Youtong Zheng<sup>1</sup>, Daniel Rosenfeld<sup>2</sup>, and Zhanqing Li<sup>1</sup>

**Affiliations:**

<sup>1</sup>Earth System Science Interdisciplinary Center, University of Maryland, College Park, Maryland, 20742, USA.

<sup>2</sup>Institute of Earth Science, Hebrew University of Jerusalem, Jerusalem, Israel.

**Contents of this file**

- 1. Text S1~S2
- 2. Figures S1~S6

**Text S1: Automatic detection of atmospheric fronts**

24 The  $F$  diagnostic is defined as:

25 
$$F = \frac{\zeta|\nabla T|}{f|\nabla T|_{ref}}$$

26 in which  $\zeta$  and  $|\nabla T|$  are isobaric relative vorticity and horizontal temperature gradient, both at  
27 900 hPa pressure level. An atmospheric front is characterized by greater values of both  
28 parameters.  $f$  and  $|\nabla T|_{ref}$  are the Coriolis parameter and reference temperature gradient, taken  
29 as 0.45 K/(100 km), respectively, which are used to normalize the  $\zeta|\nabla T|$ . A threshold  $F$  value of  
30 1 is chosen to determine frontal regions. Figure S1 shows an example of frontal systems during  
31 the MARCUS field campaign over the Southern Ocean (Zheng and Li, 2019), which illustrates  
32 the good performance of the  $F$  diagnostic in detecting frontal regions.

33

34

35

36

37

38

39

40

41

42

43

44

45

46

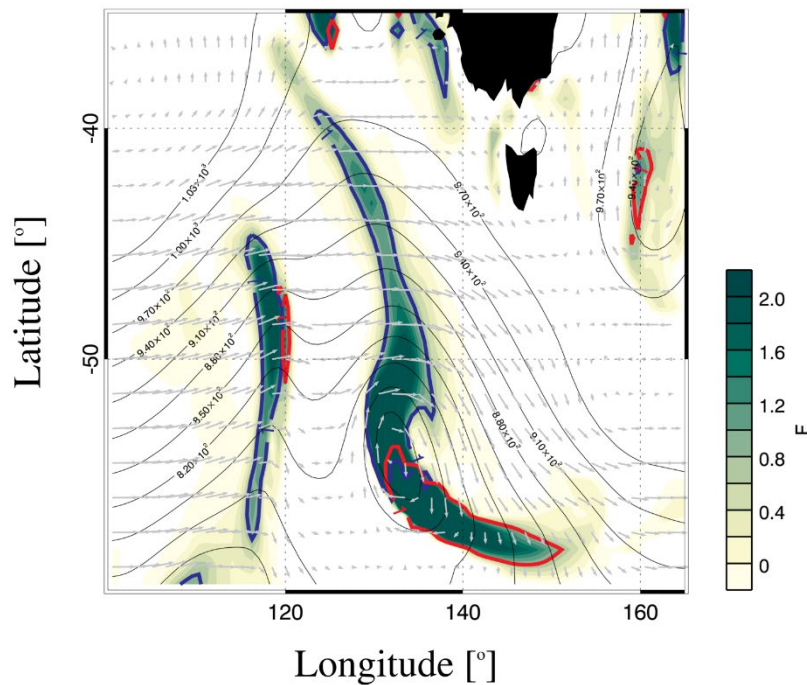
47 **Text S2: Description of the mixed-layer model**

48 The mixed-layer model (MLM) is exactly the same with that used in Bretherton and  
49 Wyant (1997). It is a 1-D model that treats a stratocumulus-topped boundary layer (STBL), from  
50 the surface to the top of the stratocumulus deck, as a bulk layer. There are two prognostic  
51 thermodynamic variables: total water mixing ratio and moist static energy, both which are  
52 assumed to be conserved in adiabatic moist convection, and are thus vertically uniform in a  
53 STBL. The MLM parameterizes the surface fluxes, radiative fluxes, precipitation fluxes, and  
54 entrainment rate. The insolation is diurnally averaged. The entrainment closure scheme is based  
55 on the amount of STBL-averaged turbulent kinetic energy, in which the entrainment rate is  
56 primarily dependent on the convective velocity scale (Turton and Nicholls, 1987). The vertical  
57 grid size is set as 10 m.

58 The initial and boundary conditions are taken from the Table 1 in Bretherton and Wyant  
59 (1997). The free-troposphere thermodynamics remain fixed and the underlying sea surface  
60 temperature increases gradually by 1.5 K/day. We modify the sea surface temperature increasing  
61 rate to 5 K/day and 10 K/day to fulfill our purpose as described in the manuscript.

62

63



64

65 **Figure S1:** An example of using the  $F$  diagnostic to identify frontal systems. The date of the case  
66 is 1 March 2018 over the Southern Ocean. The blue and red contours mark the identified cold  
67 and warm fronts, respectively.

68

69

70

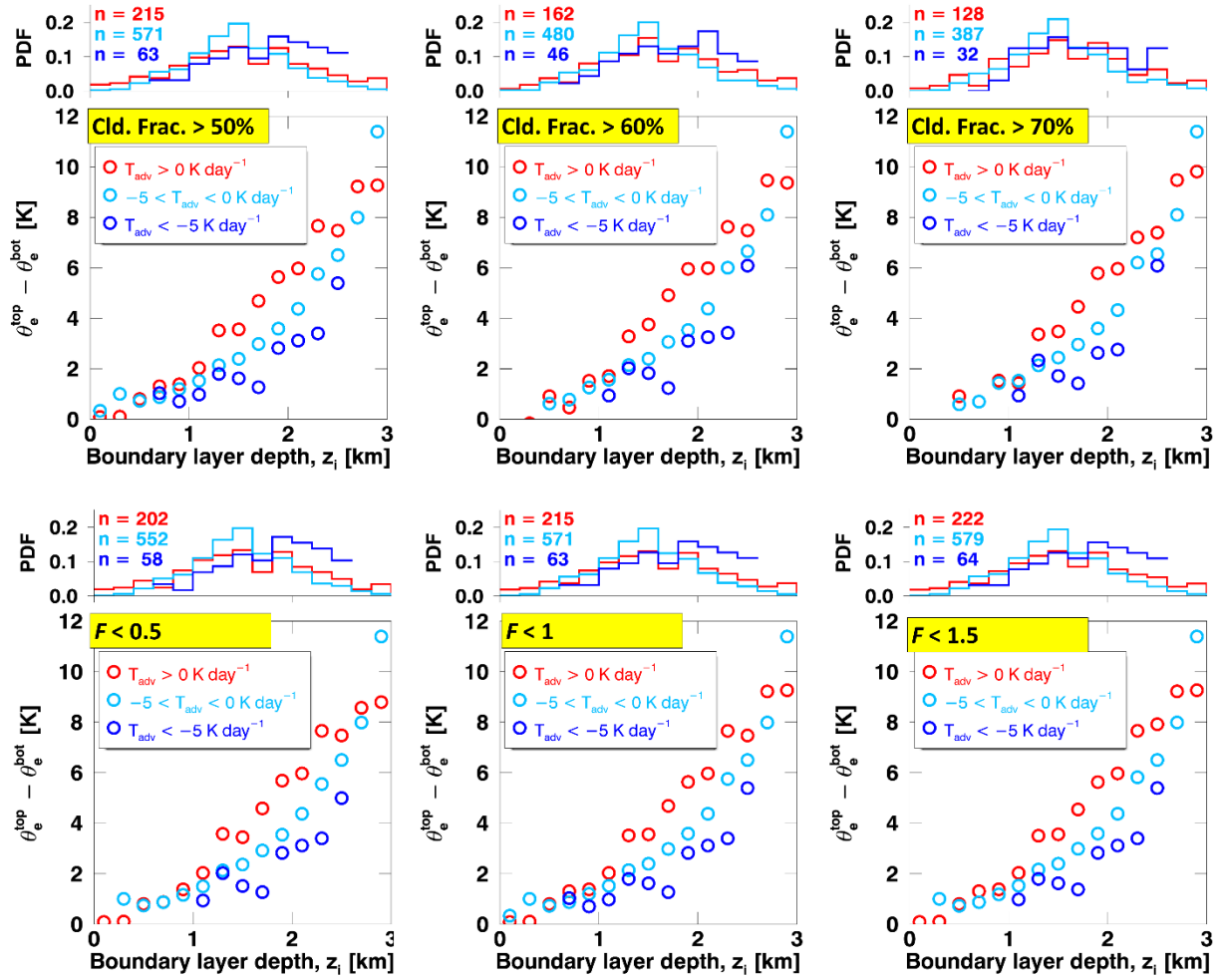
71

72

73

74

75



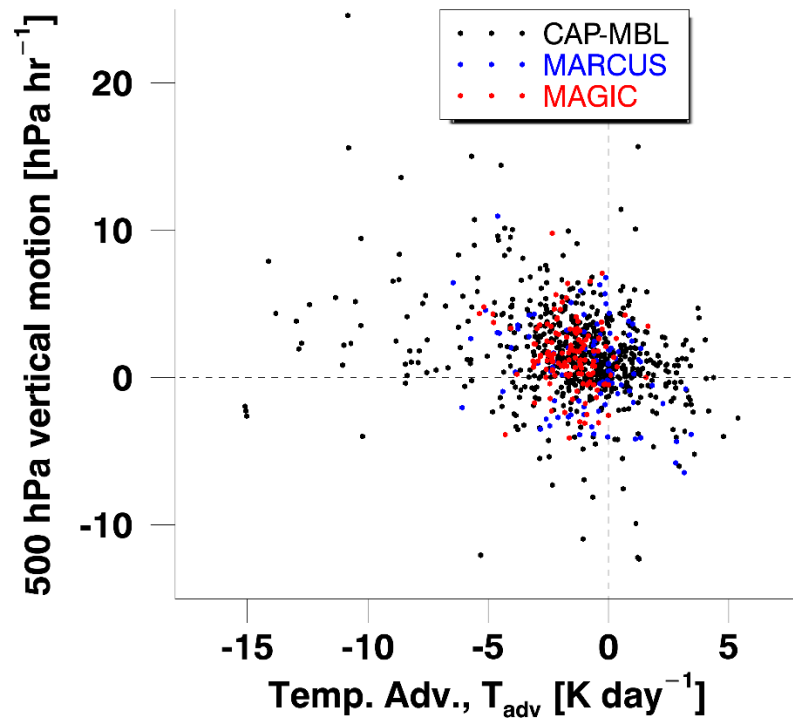
76

77 **Figure S2:** Same with Figure 1a but for STBL cases with cloud fraction greater than 50%, 60%,  
 78 and 70% (upper panel) and with  $F$  smaller than 0.5, 1, and 1.5 (bottom panel).

79

80

81



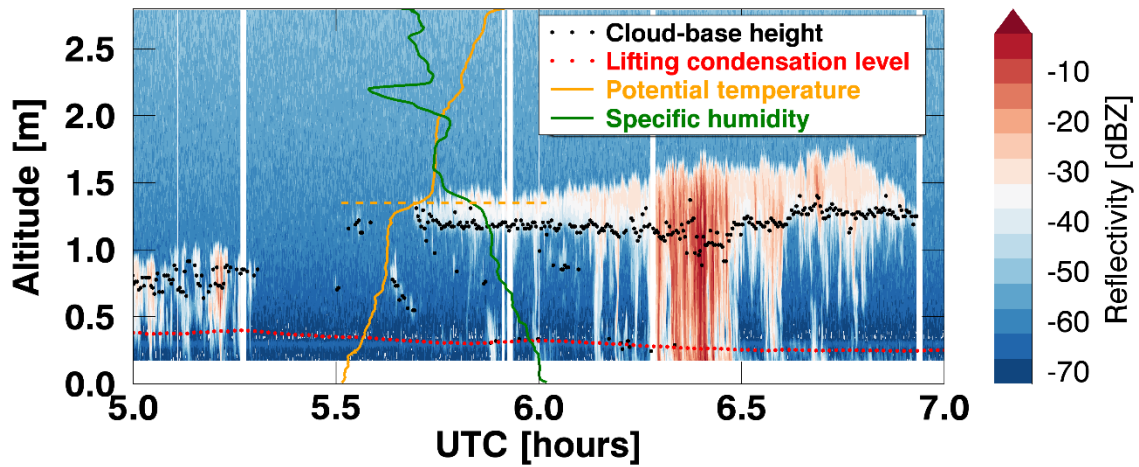
82

83 **Figure S3:** Scatterplot of the selected cases in the two-dimensional space of temperature  
84 advection and 500 hPa vertical motion.

85

86

87



88

89 **Figure S4:** (a) Height-time plot of WACR image of clouds during the CAP-MBL on May 19  
 90 2010. The sampled clouds were under the influence of warm air advection. The red and black  
 91 dots mark the lifting condensation level and ceilometer-measured cloud-base heights,

92 respectively. Orange and green lines are profiles of radiosonde-measured potential temperature  
 93 and specific humidity scaled by  $\pm 0.5$  hrs. The horizontal dashed orange line marks the identified

94  $z_i$ .

95

96

97

98

99

100

101

102

103

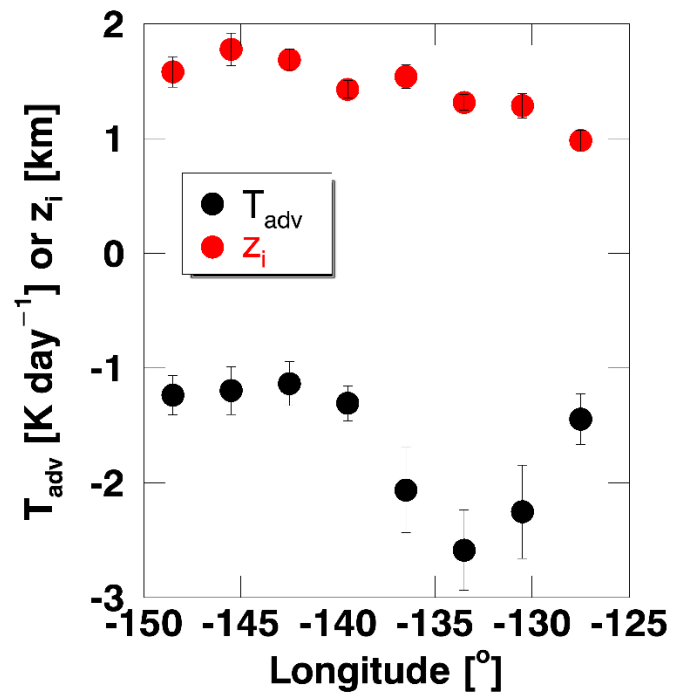
104

105

106

107

108



109

110

**Figure S5:** Variations of  $T_{adv}$  and  $z_i$  with the longitude during the MAGIC.

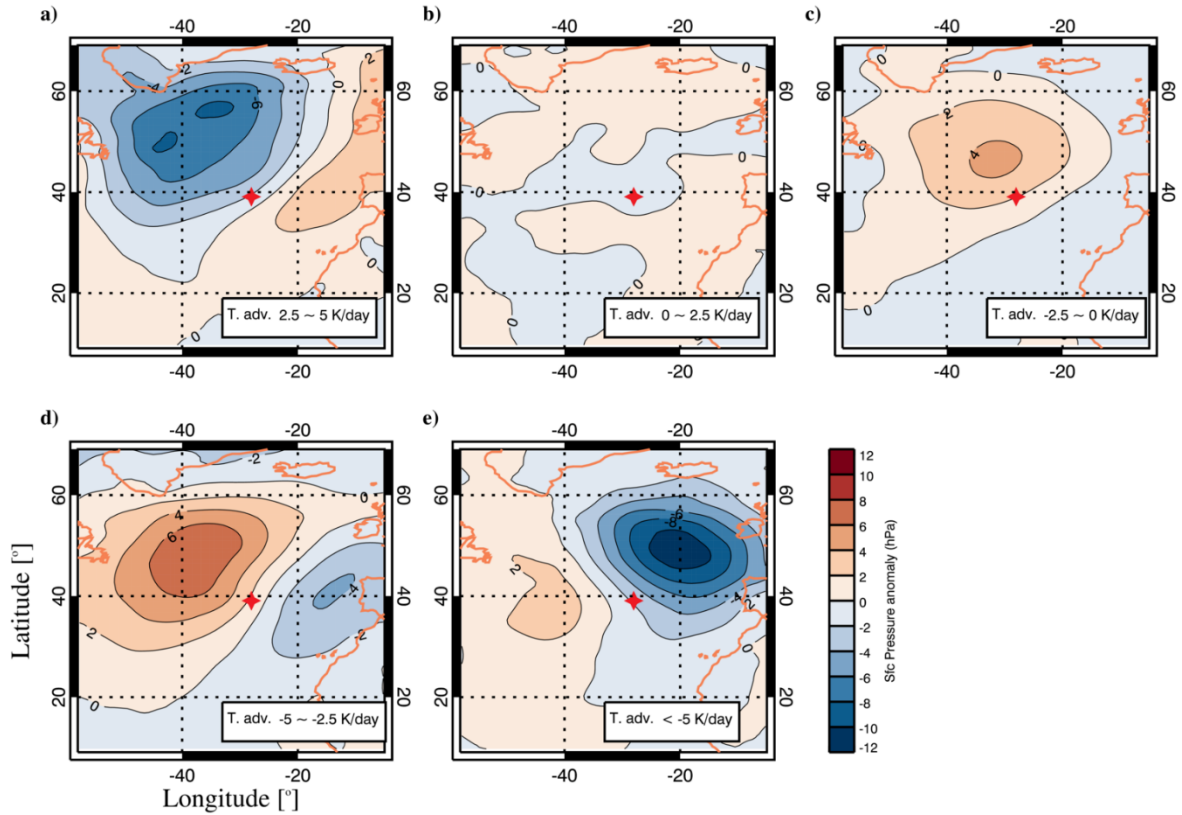
111

112

113

114

115



116

117 **Figure S6:** The composite surface pressure anomalies (relative to the monthly mean) around the  
 118 observational site on the Graciosa Island during the CAP-MBL (red star) under the influence of  
 119 temperature advection with different strengths and directions.

120

121

122

123

124

125

126

127

128 **Reference:**

129 Bretherton, C. S., & Wyant, M. C. (1997). Moisture transport, lower-tropospheric  
130 stability, and decoupling of cloud-topped boundary layers. *Journal of the atmospheric*  
131 *sciences*, 54(1), 148-167.

132 Turton, J. D., & Nicholls, S. (1987). A study of the diurnal variation of stratocumulus  
133 using a multiple mixed layer model. *Quarterly Journal of the Royal Meteorological*  
134 *Society*, 113(477), 969-1009.

135  
136 Zheng, Y., & Li, Z. (2019). Episodes of Warm-Air Advection Causing Cloud-Surface  
137 Decoupling During the MARCUS. *Journal of Geophysical Research: Atmospheres*.